Cytoskeletal and Morphologic Impact of Cellular Oxidant Injury

DANIEL B. HINSHAW, MD, LARRY A. SKLAR, PhD, BEN BOHL, BS, INGRID U. SCHRAUFSTATTER, MD, PAUL A. HYSLOP, PhD, MICHAEL W. ROSSI, PhD, ROGER G. SPRAGG, MD, and CHARLES G. COCHRANE, MD

From the Department of Immunology, Scripps Clinic and Research Foundation, La Jolla, California

The relationship between changes in cell morphology and the cytoskeleton in oxidant injury was examined in the P388D$_1$ cell line. Flow cytometry of cells stained with NBD-phallacidin, a fluorescent probe specific for filamentous (F) actin, revealed a substantial increase in F actin content in H_2O_2-injured cells over 3–4 hours. Doses of H_2O_2 as low as 500 μM produced sustained increases in F actin content. Experiments where catalase was used to interrupt H_2O_2 exposure over a long time course revealed 15–30 minutes to be the critical period of exposure to 5 mM H_2O_2 necessary for a sustained increase in F actin as well as large increases in membrane blebbing and later cell death. The increase in F actin with H_2O_2 injury was confirmed with the use of electrophoresis in acrylamide gels of 1% Triton X-100 cytoskeletal extracts from P388D$_1$ cells. Scanning electron microscopy revealed major loss of surface convolutions in addition to the formation of blebs. Fluorescence microscopy of adherent cells using rhodamine phalloidin showed considerable cell rounding and rearrangement of cellular F actin by 30 minutes of exposure to H_2O_2. Transmission electron microscopy revealed side to side aggregation of F actin bundles (microfilaments) developing during this time. Considerable swelling of mitochondria and other subcellular organelles was seen after 2 hours of injury. The apparent area of attachment to the substrate was markedly diminished in injured cells. H_2O_2 injury produced a marked increase in F actin with an associated rearrangement of the microfilaments and simultaneous changes in the plasma membrane prior to cell death in the P388D$_1$ cell line. (Am J Pathol 1986, 123:454–464)

OXIDANTS and proteases produced by stimulated polymorphonuclear leukocytes (PMNs) in areas of inflammation are associated with tissue injury. O_2^- and H_2O_2 are major oxidants produced by PMNs capable of causing cell lysis within hours after exposure.[1-5]

Several events occur with oxidant injury to cells, including 1) rapid loss of cellular adenosine triphosphate (ATP); 2) elevation of intracellular free Ca^{2+} ($[Ca^{2+}]_i$)[6]; 3) oxidation of glutathione (GSH); and 4) loss of the coenzyme NAD[7,8-10] associated with activation of polyadenosine diphosphate (poly-ADP) ribose polymerase and breaks in single-stranded DNA.[7] Injured and dying cells have been noted to undergo morphologic changes, including swelling of the cytoplasm and blebbing of the plasma membrane.[11] Membrane blebbing has been associated with changes in intracellular Ca^{2+} homeostasis and glutathione redox status.[10,12] A variety of agents including sulfhydryl-reactive alkylating agents, formaldehyde, trypsin, and drugs that induce the formation of oxidants and free radicals as byproducts of their metabolism are known to induce blebbing in different cell systems.[12-15] Apparent redistribution of cellular filamentous (F) actin has occurred in cells with blebs, including endothelial cells exposed to fibrinogen fragment D.[16-18] Increased lateral diffusion of membrane receptors associated with blebbing of the plasma membrane has been thought to reflect major alterations in the cytoskeleton of cells with blebbing.[16,17] Increases in F actin associated with major morphologic changes occur in activated platelets and stimulated polymor-

Supported in part by NIH Grant AI19032, SCOR Grant HL23584, Council for Tobacco Research Grant 7864-I, and Office of Naval Research Grant 105-837. L.A. Sklar is an established investigator of the American Heart Association with funds contributed by the California affiliate.

This is publication number 3884 IMM from the Department of Immunology.

Accepted for publication January 15, 1986.

Address reprint requests to Daniel B. Hinshaw, MD, Department of Surgery, Medical College of Virginia, Box 661—MCV Station, Richmond, VA 23298.

phonuclear leukocytes (PMNs) as well as other cell types.[19-23]

The molecular nature of the change in cell morphology seen with injury due to oxidants or other toxic substances is not clear. The role of the cytoskeleton in regulating shape change in response to injury and its relationship to membrane changes (ie, blebbing) is poorly understood. Whether or not changes in cell shape associated with oxidant injury are signs of irreversible cell damage has not been established.

In order to address these questions, we examined the effect of oxidant (H_2O_2) injury on cellular F actin content in the P388D_1 cell line. This line was chosen because extensive characterization of the biochemical sequelae of oxidant injury has already been accomplished and because these cells are readily removed from the substratum for single cell flow cytometric analysis. We performed time course experiments to examine the temporal relationship between cytoskeletal and morphologic changes induced by oxidant injury. We also examined dose response and observed the minimal exposure to oxidant necessary for sustained injury (cell death) in order to ascertain the relationship of morphologic changes induced by injury and its reversibility. Ultrastructural studies were performed to further define relationships between oxidant-induced changes in morphologic features and the cytoskeleton.

Materials and Methods

Cells and Culture

The P388D_1 murine cell line was cultured at 37 C under 5% CO_2/95% air in medium RPMI 1640 (Irvine Scientific) supplemented with 2 mM glutamine (MA Bioproducts), 10% fetal calf serum (Hyclone), and gentamicin sulfate, 0.05 mg/ml (MA Bioproducts). Cells were harvested from 150-sq cm culture flasks (Corning) by scraping with a rubber policeman and centrifuged at 1500 RPM for 5–10 minutes. Experimental protocols were carried out with cells suspended at a concentration of 2×10^6/ml in modified Gey's buffer containing in most circumstances 147 mM NaCl, 5 mM KCl, 1.9 mM KH_2PO_4, 1.1 mM Na_2HPO_4, 0.3 mM $MgSO_4$, 1 mM $MgCl_2$, 5.5 mM glucose, and 1.5 mM $CaCl_2$.

Routine cell counts were made with an hemacytometer. Cell viability was tested with trypan blue, viable cells excluding the dye. Cellular morphologic findings were assessed under the same conditions as viability, and the percentage of viable cells with membrane blebbing occurring during different experimental conditions was recorded.

Cell injury at 37 C was initiated by addition of appropriate dilutions of reagent grade hydrogen peroxide (H_2O_2, Scientific Products). Controls received equal volumes of buffer without H_2O_2. In some experiments bovine catalase (Sigma Chemical Co.), 2500 U/ml of cell suspension, was added at different time points to remove H_2O_2. Using a fluorimetric assay[24] for H_2O_2, we determined that addition of this amount of catalase did remove all measurable oxidant upon addition.

NBD-Phallacidin Staining

NBD-phallacidin, a fluorescent derivative of the phallotoxin from *Amanita phalloides*, which binds with high affinity to F actin, has been adapted recently for use in assaying cellular F actin by flow cytometry.[20,21,23,25,26]

With a method adapted from Howard and Meyer[20] 2×10^6 cells (1 ml of cell suspension) were centrifuged in a Beckman Microfuge at ⅓ maximal speed for 10 seconds. The pellet was resuspended in 0.9 ml of modified Gey's buffer and combined with 0.1 ml of a solution made up of equal aliquots of 3.3 μM NBD-phallacidin (Molecular Probes) and 1 mg/ml lysophosphatidyl choline (Sigma Chemical Co.) in 37% phosphate-buffered formalin. Samples were then incubated at 37 C for at least 10 minutes. Stained samples were stable for at least a week after staining when left unwashed.

Flow Cytometric Analysis

NBD-phallacidin staining of F actin was demonstrated on the FACS IV (Becton Dickinson) with fluorescence excitation by argon laser at 488 nm and emission at 522 nm. Results were stored as histograms or dot plots of fluorescence, forward angle, and side scatter on floppy disk or in list mode in a computer (Consort 30, Becton Dickinson) for further analysis. Data presented represents total ungated populations of the cells studied. Cytometric comparisons between control and injured populations were made by setting control cells at the midrange of fluorescence. Departures from this control midrange represent changes in relative fluorescence (ie, NBD-phallacidin binding or F actin content).

Triton X-100 Cytoskeleton Analysis

The method of Phillips et al[19] was adapted for use with modified Gey's buffer as follows: cells at 2×10^6/ml were incubated $\pm H_2O_2$ at 37 C for various intervals; 5 or 10 ml of cell suspension ($1–2 \times 10^7$ cells) was centrifuged at 1500 RPM for 5–10 minutes; the pellet was resuspended in 0.5 ml of buffer to which 0.5 ml 2% Triton X-100 was added for a final 1% Triton X-100 concentration; the samples were allowed to sit at

room temperature for 5 minutes and then centrifuged for 4 minutes at high speed (8000*g*) in a Microfuge (Beckman); the supernatant was discarded and the pellet again washed with 1% Triton X-100 without resuspension; the washed pellet was boiled at 100 C in 2% SDS ±2% vol/vol β-mercaptoethanol for 15 minutes; samples were then run on 11% sodium dodecyl sulfate polyacrylamide gel electrophoresis (SDS-PAGE) after the method of Laemmli.[27]

High-molecular-weight standards including 45,000 mol wt and purified rabbit skeletal muscle F actin[28] were run along with the samples for identification of sample F actin. Visual inspection of Coomassie blue-stained gels usually demonstrated differences between sample quantities of F actin, which were also confirmed by densitometric scanning.

Scanning Electron Microscopy (SEM)

After incubation at 2 × 10^6 cells/ml with or without 5 mM H_2O_2 at 37 C for 90 minutes, the cells were fixed with modified Karnovsky's fixative (1.5% glutaraldehyde, 2% paraformaldehyde in 0.1 M cacodylate buffer, pH 7.4) for 1–2 hours at 4 C. They were postfixed with 1% osmium tetroxide in the same buffer for 1 hour at room temperature. The suspended cells were allowed to adhere to a 12-mm round glass coverslip which was precoated with poly-L-lysine. The coverslips with adherent cells were dehydrated through graded ethanol and critical-point-dried in a Bomar SPC-900 critical-point drier and sputter-coated with a carbon target in a Technics sputter coater. The cells were viewed with an Hitachi S-500 scanning electron microscope at 20,000 acceleration voltage.

Fluorescence Microscopy

Cells grown overnight on glass coverslips or plastic Petri dishes at 2 × 10^5 cells/cm^2 were exposed in full culture media to buffer or H_2O_2 (5 mM); the cells were later washed and then fixed, permeabilized, and stained with rhodamine phalloidin. The cells were then in-

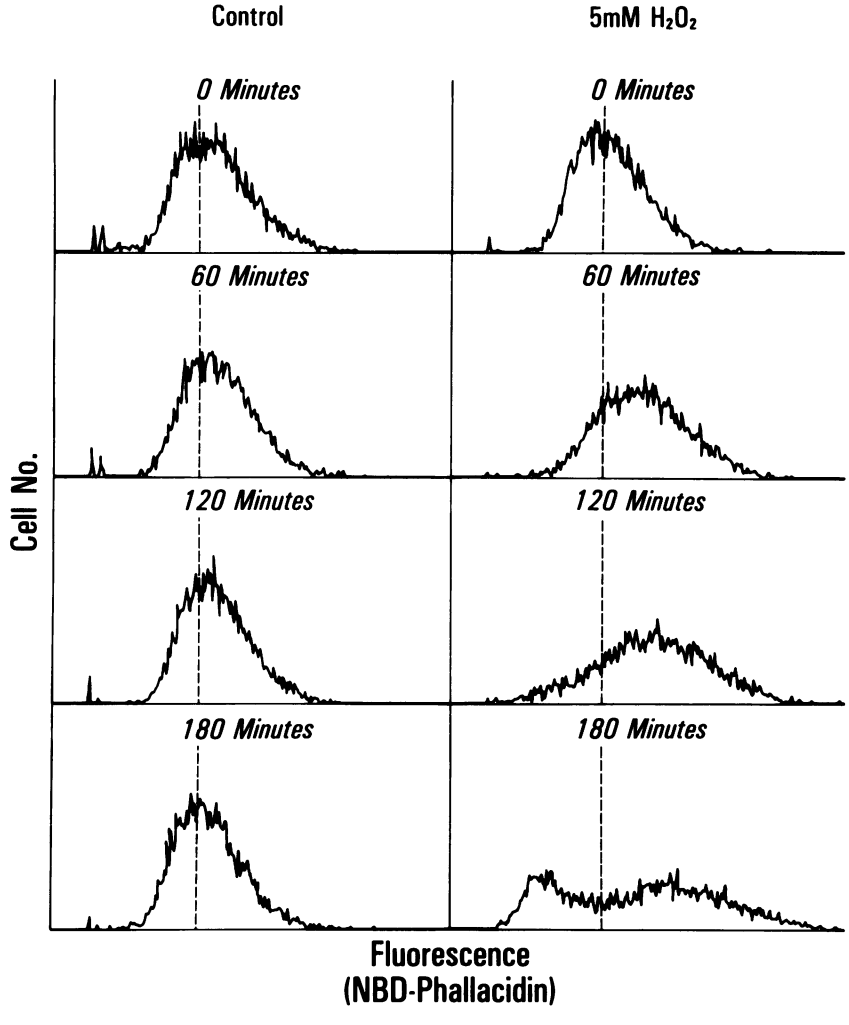

Figure 1—The time course of actin polymerization in P388D$_1$ cells ± 5 mM H_2O_2 measured by FACS analysis of NBD-phallacidin-stained cells. Data are from a representative experiment repeated at least three times. *Dashed vertical lines* represent mean fluorescence of reference samples at the beginning of the time course. Note the appearance of the second low fluorescence peak in the 180-minute H_2O_2 sample.

cubated for at least 10 minutes at 37 C with the staining buffer prior to fluorescence microscopy. Phase-contrast and fluorescent micrographs were taken at 400× magnification using Tri X Pan film (Kodak) on a Zeiss fluorescence microscope.

Transmission Electron Microscopy (TEM)

Cells grown up overnight on plastic Petri dishes were exposed to 5 mM H_2O_2 for varying times over a 2-hour time course. After a brief wash with modified Gey's buffer, the cells were fixed as above. The cells were dehydrated through graded ethanol and flat-embedded in Epon 812. Blocks were cut on a LKB Ultramicrotome III parallel or perpendicular to the plane of the substratum. Silver to light gold sections were mounted on bare grids, stained with uranyl acetate and lead citrate, and viewed with a Hitachi HU 12A electron microscope at 75,000 accelerating voltage.

Results

Cytometric Analysis of the Time Course of Blebbing and Actin Polymerization

The time course of cell injury over 3 hours with exposure to a single bolus of 5 mM H_2O_2 was assessed by FACS analysis of cells stained with NBD-phallacidin at different time points. F actin content as measured by increasing fluorescence in three experiments steadily increased over the time course (Figure 1). This represented a relative increase in the F actin content of approximately 150%, compared with the level in control, uninjured cells. Simultaneously, a change occurred in the size distribution of the injured cell population, and increasing numbers of a small low fluorescence population became prominent by 3 hours. Analysis of forward angle scatter (size) versus fluorescence data from a similar experiment revealed that the growing population of low fluorescence (low F actin content) was also very small in size. (Figure 2). The splitting of the origi-

Table 1—Time Course of Viability and Membrane Blebbing in P388D$_1$ Cells Injured With 5 mM H_2O_2

	% Viability (trypan blue exclusion) (n = 5)	% Viable cells with blebbing (n = 5)
0 minutes H_2O_2	88 ± 1.5*	0.4 ± 0.25
60 minutes H_2O_2	87.6 ± 2.7	15.6 ± 6.22
120 minutes H_2O_2	61 ± 11.7	35.4 ± 10.29
180 minutes H_2O_2	54.2 ± 10.6	41 ± 6.62

* Standard error of the mean.

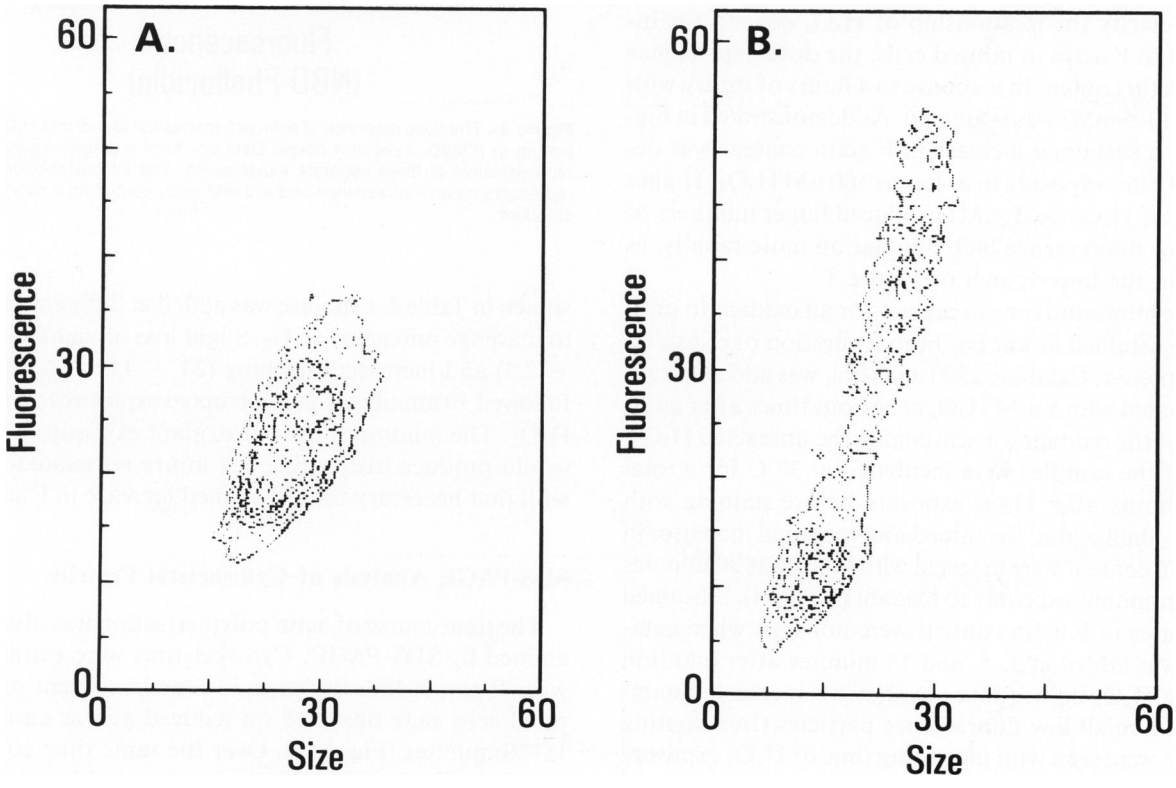

Figure 2—Contour graph of dot plot distribution of P388D$_1$ cells at 4 hours ± 5 mM H_2O_2. **A**—Control pattern. **B**—Injured pattern. Note the two distinct populations: 1) decreased in size and fluorescence compared with the control population; 2) increased in fluorescence compared with the control population.

nal population into two seen by flow cytometry reflected the release of blebs from injured cells. The uninjured controls demonstrated very little change in their F actin content or size distribution over the same time course (Figures 1 and 2). The mean size of the smaller population was approximately half that of the larger population. Free-floating blebs visualized by light microscopy were almost half the size of the parent cells.

Microscopic Analysis of Blebbing

In order to assess the temporal relationship between the increase in F actin content seen by FACS analysis of NBD-phallacidin-stained cells and associated morphologic changes due to oxidant injury, we studied cells with or without H_2O_2 exposure over a similar time course. Cell membrane blebbing observed by light microscopy preceded the loss of viability by trypan blue exclusion (Table 1). The blebbing steadily increased over time with eventual release of the blebs from the injured cells at late time points (3–4 hours). Maximal blebbing occurred late in the time course in 30–50% of viable cells, because many cells had released blebs by this time.

Dependence of F Actin Content on the Dose of H_2O_2 and the Period of Injury

To clarify the relationship of H_2O_2 dose to the increase in F actin in injured cells, the dose dependence of F actin content in response to 4 hours of injury with H_2O_2 (0–5 mM) was examined. As demonstrated in Figure 3, a sustained increase in F actin content was detected after exposure to as low as 500 μM H_2O_2. Higher doses of H_2O_2 (ie, 5 mM) produced larger numbers of the low fluorescence bleb population more rapidly, as seen in the lower panel of Figure 3.

The minimum time necessary for an oxidant to initiate a sustained injury has been a question of considerable interest. Catalase, 2500 units/ml, was added to cells incubated with 5 mM H_2O_2 at various times after addition of the oxidant for scavenging the unreacted H_2O_2. All of the samples were incubated at 37 C for a total of 4 hours after H_2O_2 exposure before staining with NBD-phallacidin. Sustained and maximal increases in F actin content were detected with as little as 30 minutes of continuous exposure to oxidant (Figure 4). Sustained increases in F actin content were not seen when catalase was added at 1, 5, and 15 minutes after addition of the H_2O_2 bolus (data not shown). Increasing numbers of small low fluorescence particles (free floating blebs) were seen with increasing time of H_2O_2 exposure beyond 30 minutes.

Representative data regarding viability and membrane blebbing 4 hours after oxidant exposure are shown in Table 2. Catalase was added at different times to scavenge unreacted H_2O_2. Slight loss of viability (86 ± 2.5) and increased blebbing (23 ± 4.6) at 4 hours, followed 30 minutes of uninterrupted exposure to 5 mM H_2O_2. The minimum time of oxidant exposure which would produce irreversible cell injury correlated well with that necessary for a sustained increase in F actin.

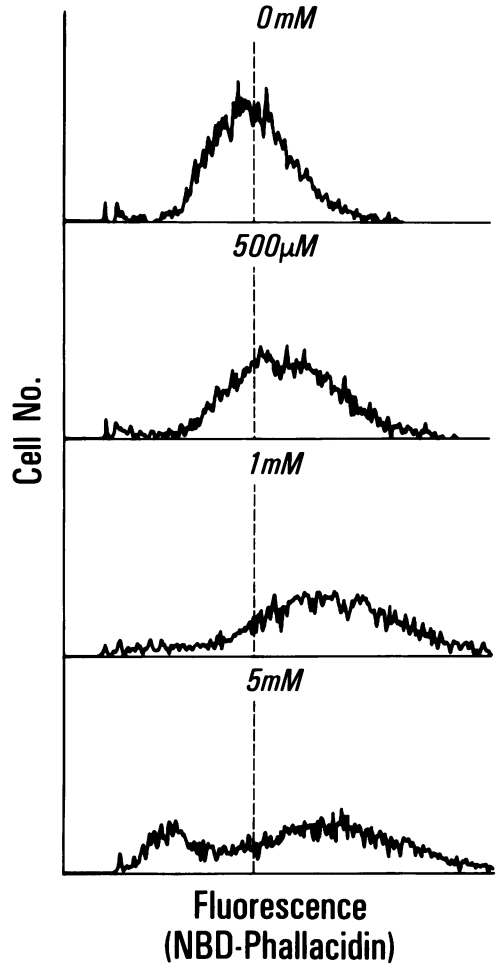

Figure 3—The dose response of actin polymerization to 0–5 mM H_2O_2 exposure in P388D$_1$ cells at 4 hours. Data are from a single experiment representative of three separate experiments. The *vertical dashed line* represents mean fluorescence of the 0 mM H_2O_2 control as a reference standard.

SDS-PAGE Analysis of Cytoskeletal Proteins

The time course of actin polymerization was also examined by SDS-PAGE. Cytoskeletons were extracted with Triton X-100. Increases in F actin content of injured cells were observed on reduced gels as early as 15–30 minutes (Figure 5). Over the same time course cytoskeletal extracts analyzed on nonreduced gels showed increasing amounts of aggregated proteins, which did not enter the gel, associated with H_2O_2 in-

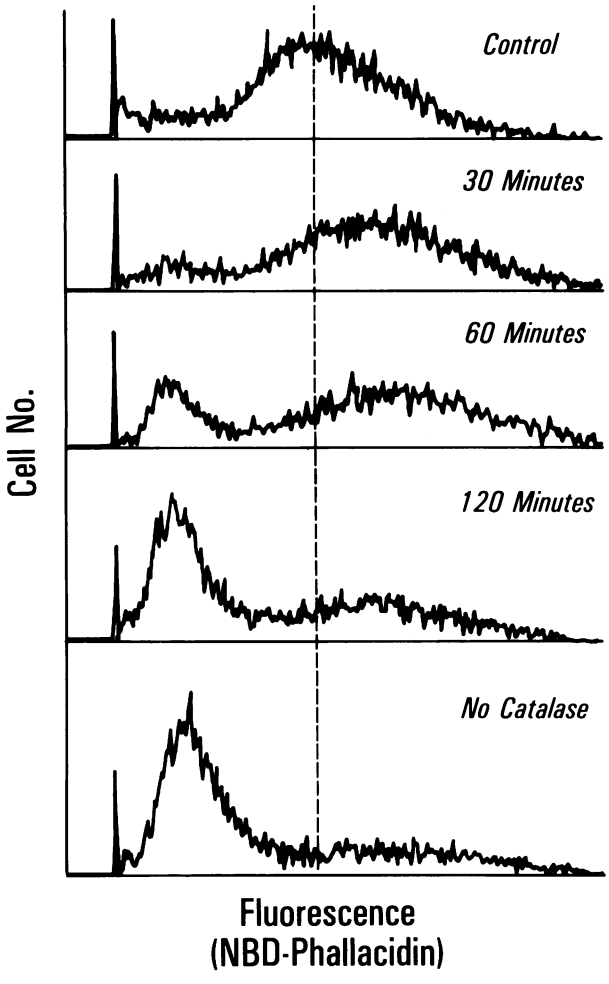

Figure 4—F actin content 4 hours after 5 mM H_2O_2 addition versus the time of catalase addition in P388D$_1$ cells. Data are from a single experiment representative of three separate repetitions. The *vertical dashed line* represents mean fluorescence of uninjured control cells as a reference standard. Note the increasing size of the low fluorescence peak seen with increasing length of exposure to H_2O_2.

jury. The increase in cytoskeletal protein seen in Triton X-100 extracts of H_2O_2-injured cells was not limited to F actin alone. Most of the protein bands stained more intensely with Coomassie blue in cytoskeletal extracts from injured cells.

Scanning Electron Microscopy

To better visualize the surface changes in oxidant injured cells associated with the blebbing of the plasma membrane, we performed scanning electron microscopy on cell suspensions (2×10^6 cell/ml). After 90 minutes' exposure to 5 mM H_2O_2, extensive changes were seen in surface morphology in the majority of cells examined (Figure 6). There was loss of the highly convoluted surface pattern seen in control cells. This was replaced with a few dominant large blebs on an otherwise smooth surface.

Fluorescence Microscopic Observations of Adherent Cells

The effect of oxidant injury on the cytoskeleton of adherent cells was next studied. Adherent cells on glass coverslips demonstrated rounding of the majority (>90%) of cells seen as early as 30 minutes after exposure to 5 mM H_2O_2 (Figure 7). An associated shortening and thickening of fluorescent rhodamine phalloidin-stained microfilaments was seen in the injured cells that had undergone rounding. Prominent F-actin-rich "spiny" projections were all that remained of cytoplasmic processes present before oxidant exposure. Later time points (1 and 2 hours) revealed persistent cell rounding among injured cells. Emerging blebs were observed to be weakly stained and free of actin filaments.

Transmission Electron Microscopic Study of Adherent Cells

Transmission electron microscopy was used to determine ultrastructural changes associated with 5 mM H_2O_2 exposure over a 2-hour time course in adherent cells (Figure 8). It revealed the formation of large bundled (parallel) side-to-side aggregates of F actin in injured cells. The aggregates were visible as early as 30 minutes after addition of H_2O_2 and were more prominent at 2 hours. Other oxidant-induced ultrastructural changes were noted after 2 hours of injury. They included swelling of the mitochondria, smooth endoplasmic reticulum, and loss of microtubules. Also, loss of plasma membrane segments was seen in cells which had presumably blebbed. Cross-sections of cells attached to the plastic substrate revealed substantial decreases

Table 2—Viability and Membrane Blebbing at 4 Hours in P388D$_1$ Cells ± 5 mM H_2O_2 Versus Time of Catalase Addition

	% Viability (trypan blue exclusion)	% Viable cells with blebbing
Control	89 ± 2.6* (n = 3)	8.3 ± .87 (n = 3)
Addition of catalase at		
1 min	89.7 ± 1.7 (n = 3)	7.7 ± 1.8 (n = 3)
5 min	88 ± 2.1 (n = 3)	8 ± 2.3 (n = 3)
15 min	87.3 ± 2.4 (n = 3)	9 ± 4.0 (n = 3)
30 min	86 ± 2.5 (n = 3)	23 ± 4.6 (n = 3)
60 min	73.2 ± 4.0 (n = 4)	26 ± 4.4 (n = 4)
No catalase	62 ± 7.2 (n = 4)	36 ± 3.4 (n = 4)

* Standard error of the mean.

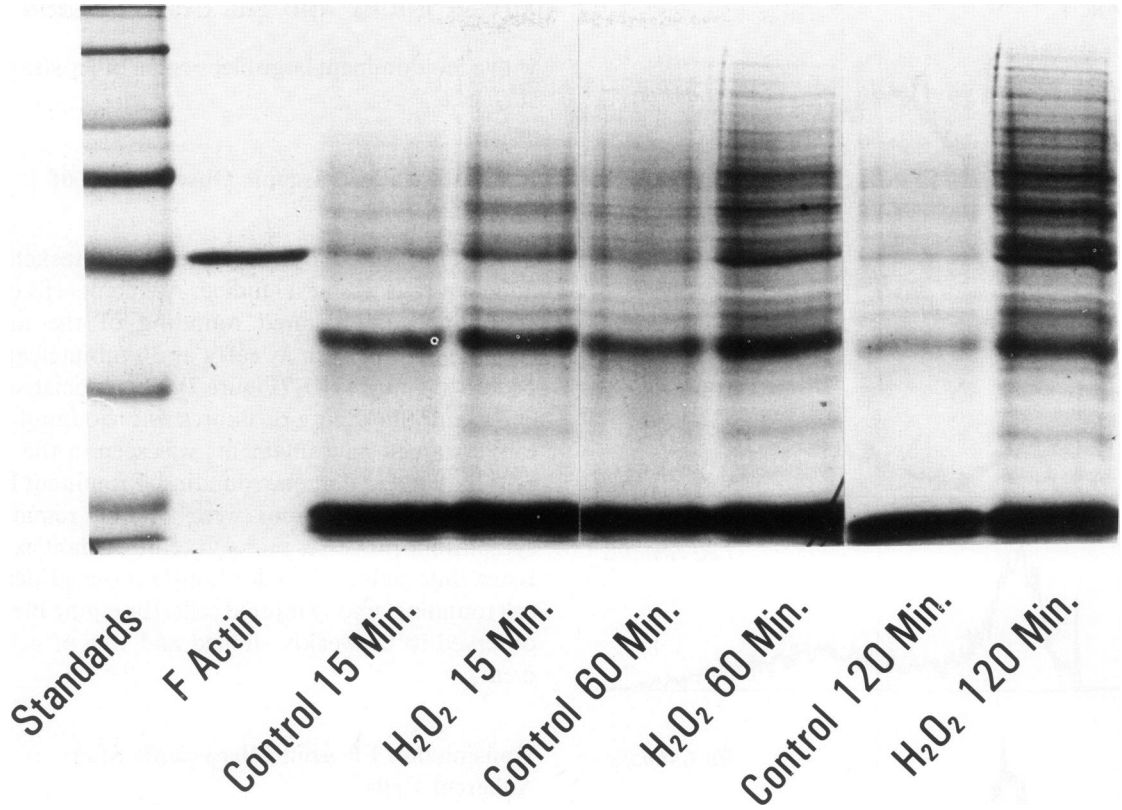

Figure 5—Eleven percent SDS-PAGE of 1% Triton X-100 cytoskeletal extracts from 2 × 10^7 P388D_1 cells per lane (reducing conditions). The samples were taken over a time course of exposure to 5 mM H_2O_2.

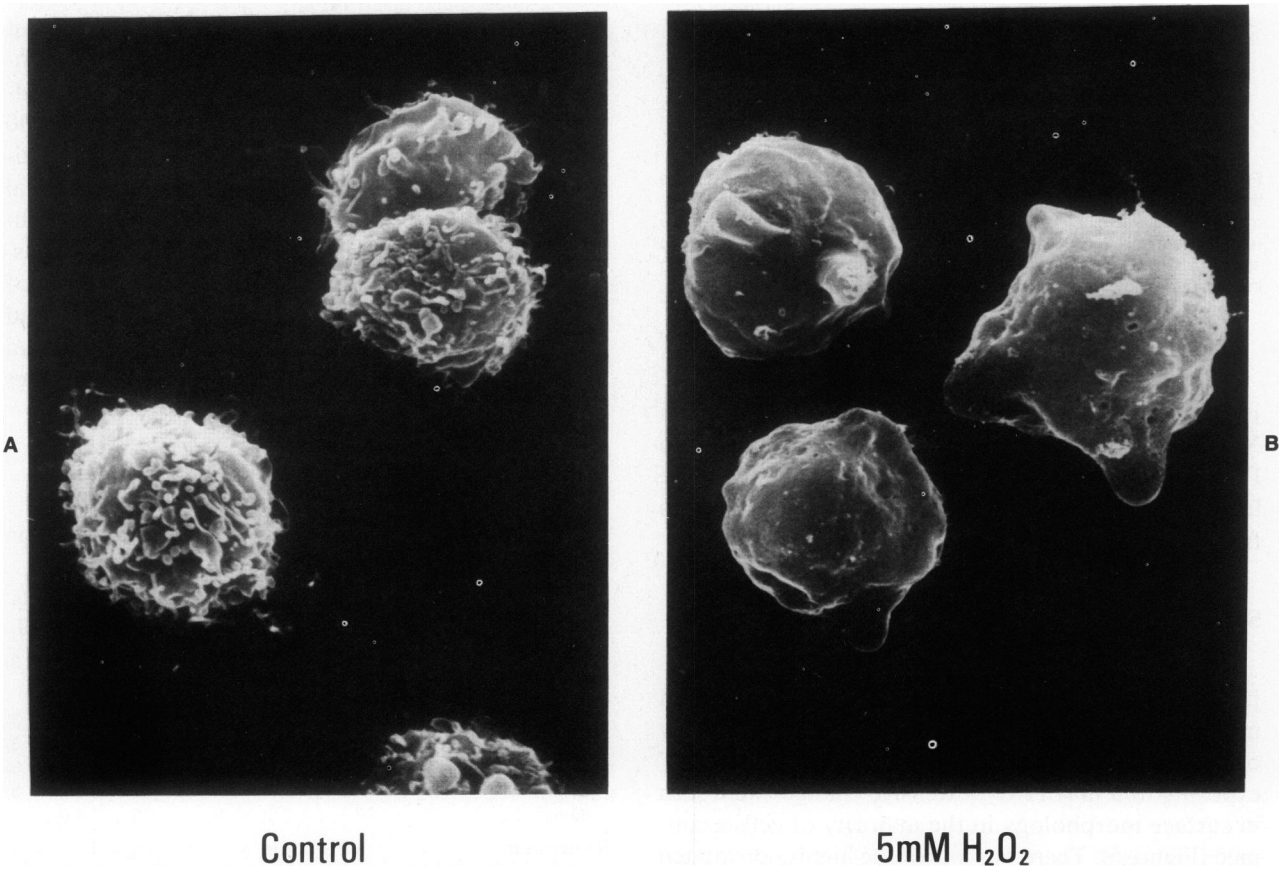

Figure 6—Scanning electron micrograph of P388D_1 cells. **A**—Control (uninjured) cells at 90 minutes after the beginning of the experiment. (×2000) **B**—Injured cells at 90 minutes of exposure to 5 mM H_2O_2. (×2000)

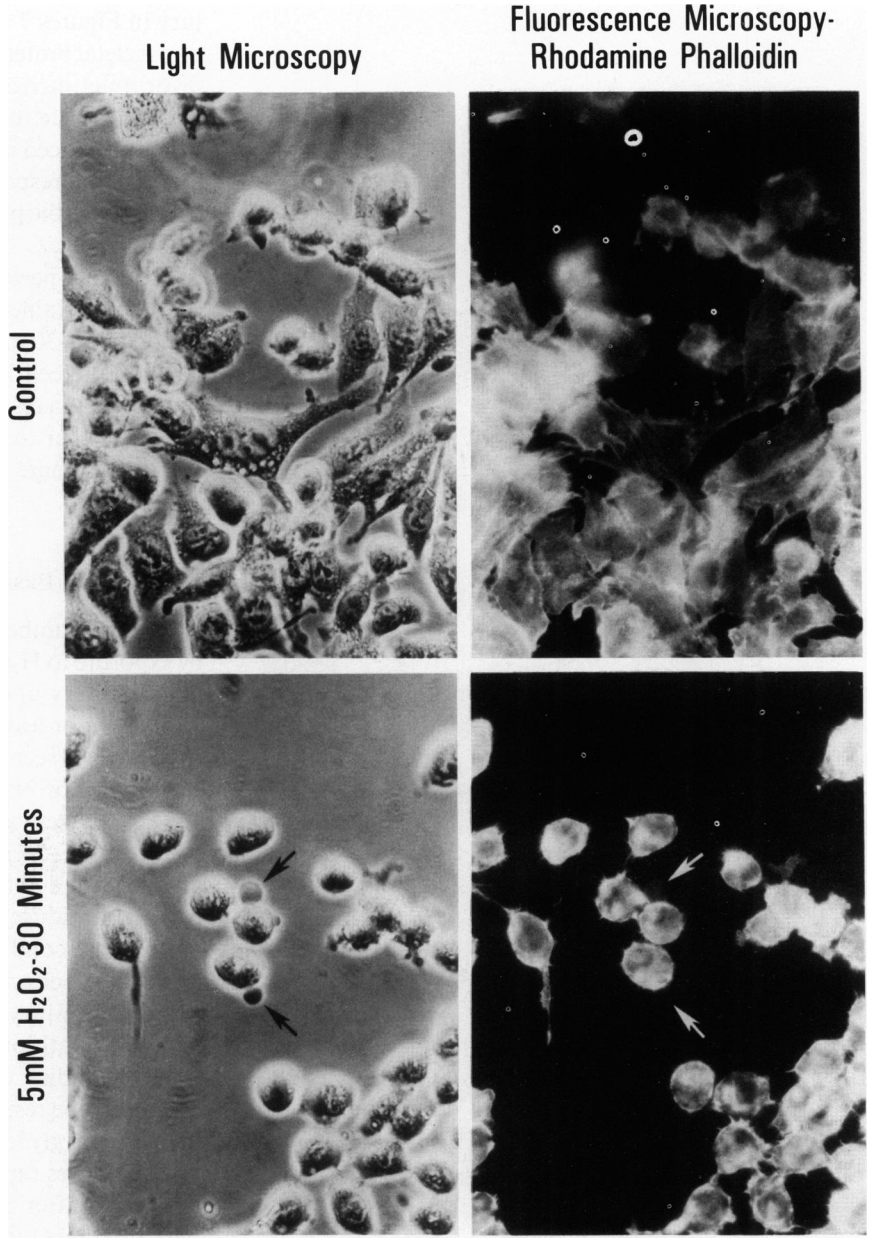

Figure 7—Light and fluorescence microscopy of adherent cells ± 5 mM H_2O_2 stained with rhodamine phalloidin. The *arrows* in the lower panels point to surface blebs on injured cells. (×400)

in the apparent surface area of attachment in cells injured for 2 hours.

Discussion

H_2O_2 Induced Injury

H_2O_2 is capable of inducing gross morphologic changes (blebbing of the plasma membrane and cell rounding) and apparent increases in F actin in a dose- and time-dependent manner in P388D_1 cells. The actual time of oxidant exposure necessary to produce sustained effects is relatively short.

Analysis of NBD-phallacidin-stained cells by flow cytometry (FACS) provides a convenient method of following the kinetics of changes in the cytoskeleton induced by oxidants. Since analysis of the cells by flow cytometry required a single cell suspension, it became necessary to use a cell line such as P388D_1, which fulfilled this criterion. It will be important in the future to develop a means of analyzing cells which form monolayers, perhaps by growing them on microcarrier beads small enough to pass through the nozzle of the flow cytometer and be analyzed as single particles.

The time course of increasing F actin content in relation to oxidant exposure is considerably slower than

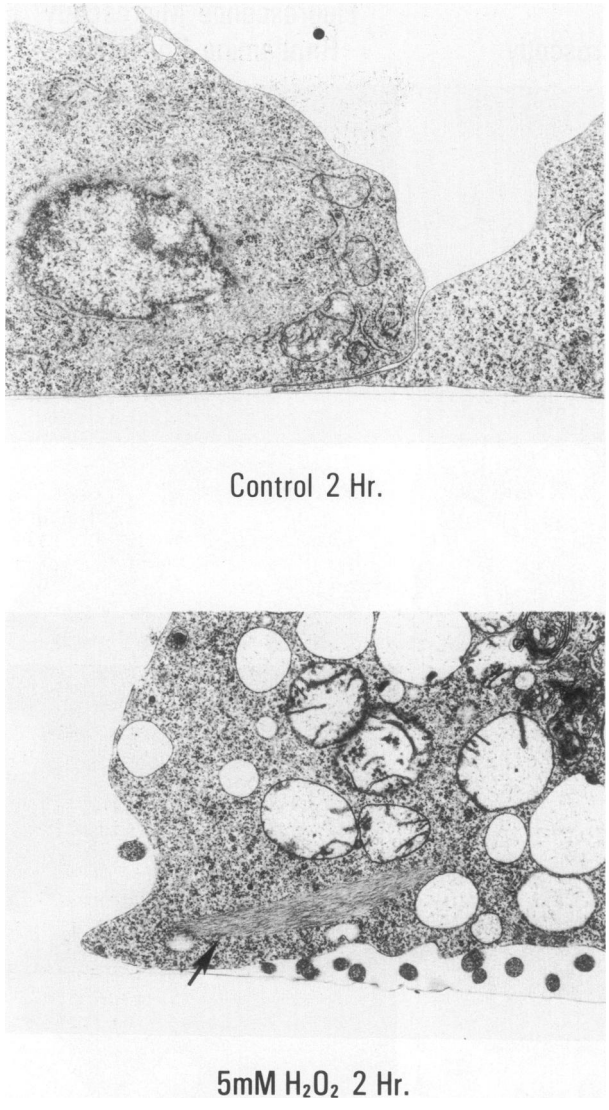

Figure 8—Transmission electron micrographs of cross-sections of adherent cells ± 5 mM H_2O_2 at 2 hours after addition of oxidant. The *arrow* in the lower panel points to an aggregate of F actin. (× 12,000)

that seen in cells stimulated with ligands (eg, chemotactic peptide).[20,21,23] However, once initiated, the changes in F actin associated with oxidant injury appear to be essentially irreversible, whereas the changes in F actin induced by ligands are transient and reversible.[20,21,23] This is consistent with other metabolic events associated with irreversible cellular injury (eg, loss of intracellular cation regulation). Transient changes in F actin associated with nonlethal oxidant injury may occur, however, and require further study.

The observed increase in many cytoskeletal associated proteins seen by SDS-PAGE of triton extracts from oxidant injured cells is similar to that seen in thrombin-stimulated platelets.[19] The apparent shortening and reorganization of microfilaments seen with oxidant injury in Figures 7 and 8 suggests that fragmentation of cytoskeletal proteins may be occurring and that this may favor a net increase in phallotoxin binding to F actin without a true increase in actin polymerization. This oxidant-induced reorganization of cytoskeletal proteins may also be responsible for increasing the amount of triton-insoluble protein in the cell, possibly by disulfide cross-linking.

The short period of oxidant exposure necessary to produce sustained injury points to an early critical period of 20–30 minutes, during which the ultimate survival of the cell is determined. The metabolic events occurring as a result of oxidant injury during this early period appear to be the determining factors concerning the ultimate changes seen in cellular shape and cytoskeleton.

Biochemical Basis of Oxidant Injury

A large number of biochemical events are affected by exposure to H_2O_2. Cellular ATP falls transiently with later recovery upon exposure to H_2O_2 concentrations of 100 μM or less. Persistent loss of ATP (<10% control levels) is seen with 500 μM H_2O_2 or greater within 15 minutes of exposure to the oxidant.[8]

There is activation of the hexose monophosphate shunt for 15–30 minutes after oxidant exposure with an associated increase in activity of the glutathione cycle.[9] In addition to the oxidation of NADPH seen under these conditions, there is a very rapid fall in levels of the coenzyme NADPH in the first few minutes of oxidant injury which is independent of the activity of the glutathione cycle.[9] Increased activity of the NAD degrading enzyme poly-ADP ribose polymerase appears to be responsible for the fall in this important cofactor of glycolysis.[7,9]

$[Ca^{2+}]_i$ rises rapidly from resting levels of 100 nM to >1500 nM after 60 minutes of H_2O_2 (5 mM) injury as measured by Quin 2 fluorescence in these same cells.[6] The increase in $[Ca^{2+}]_i$ is followed rapidly by the appearance of membrane blebbing. The blebbing has been associated with loss of normal $[Ca^{2+}]_i$ homeostasis.[10,12]

Cell swelling and membrane blebbing have been thought to be part of the process of cell death after injury.[11] Blebbing studied in other model systems has been related to alterations in the cytoskeleton.[16,17] There also appears to be a strong kinetic association between the loss of $[Ca^{2+}]_i$ regulation and subsequent membrane blebbing. Intact $[Ca^{2+}]_i$ regulation and ATP levels are necessary for normal excitation-contraction coupling of actin and myosin.[29] A situation where, simultaneously, $[Ca^{2+}]_i$ rises markedly and intracellular ATP falls may favor the stabilization of actin–myosin rigor complexes. Sustained contraction of actin–my-

osin complexes may tend to dissociate the cytoskeleton from the plasma membrane allowing bleb formation. This kind of mechanism could account for the increased lateral diffusion of membrane proteins in blebbed cells seen by others.[16,17]

The loss of fine structural detail in plasma membranes of oxidant injured cells visualized by scanning electron microscopy is also consistent with gross alterations of normal cytoskeleton–membrane interactions. Cell rounding seen as early as 30 minutes after H_2O_2 exposure shows good temporal correlation with the changes in F actin. The side to side aggregation of F actin visualized by transmission EM could be a major determinant of the associated cell shape change. Others, however, have shown that depletion of cellular ATP levels led to disruption of the microfilaments without concomitant changes in cell shape (i.e. rounding and membrane blebbing).[30-32] These observations suggest the possible involvement of other cytoskeletal structures in the shape change seen with oxidant injury. Microtubule depolymerization occurs on exposure to elevated Ca^{++} levels and may contribute to the cell rounding seen in these experiments.[33,34]

We are currently examining the effect of oxidant injury on microtubules and the role changes in cellular ATP, calcium, and thiol redox may play in the mechanism of cytoskeletal and morphologic changes induced by H_2O_2 injury to cells. Preliminary observations suggest that other toxins may also induce cytoskeletal reorganization. We found that the metabolic inhibitors 2-deoxyglucose and oligomycin, used at concentrations which completely suppress glycolytic and mitochondrial ATP synthesis, respectively, lead to about one-third of the increase of F actin staining seen with 5 mM H_2O_2.

What impact these oxidant-induced changes in cell morphology and the cytoskeleton might have on the functional characteristics of a monolayer of cells is an interesting question. Conditions including Ca^{2+} ionophore exposure, cytochalasin treatment and thiol oxidation which were associated with altered homeostasis of cytoskeletal elements, have been shown to affect the integrity of endothelial cell monolayers acting as permeability barriers in model systems.[35-37] The changes induced by oxidant in the shape and cytoskeleton of injured cells may also destroy the functional integrity of surfaces made up of intact monolayers of cells (eg, capillary endothelium). Whether or not oxidant-injured cells are more susceptible to a second injury remains to be determined.

References

1. Nathan CF, Silverstein SC, Breckner LH, Cohn ZA: Extracellular cytolysis by activated macrophages and granulocytes: II. Hydrogen peroxide as a mediator of cytotoxicity. J Exp Med 1979, 149:100–113
2. Simon RH, Scoggin CH, Patternson D: Hydrogen peroxide causes the fatal injury to human fibroblasts exposed to oxygen radicals. J Biol Chem 1981, 256:7181–7186
3. Weiss SJ, Young J, LoBuglio AF, Slivka A: Role of hydrogen peroxide in neutrophil-mediated destruction of cultured endothelial cells. J Clin Invest 1981, 68:714–724
4. Sacks T, Moldow CF, Craddock PR, Bowers TK, Jacobs HS: Oxygen radicals mediate endothelial cell damage by complement-stimulated granulocytes: An in vitro model of immune vascular damage. J Clin Invest 1978, 61: 1161–1167
5. Martin WJ II: Neutrophils kill pulmonary endothelial cells by a hydrogen peroxide dependent pathway. Am Rev Respir Dis 1984, 130:209–213
6. Hyslop PA, Hinshaw DB, Schraufstatter IU, Sklar LA, Spragg RG, Cochrane CG: Intracellular calcium homeostasis during hydrogen peroxide injury to cultured $P388D_1$ cells. (Manuscript submitted)
7. Schraufstatter IU, Hinshaw DB, Hyslop PA, Spragg RG, Cochrane CG: Oxidant injury of cells: DNA strand breaks activate polyadenosine diphosphate-ribose polymerase and lead to depletion of nicotinamide adenine dinucleotide. J Clin Invest 1986, 77:1312–1320
8. Spragg RG, Hinshaw DB, Hyslop PA, Schraufstatter IU, Cochrane CG: Alterations in adenosine triphosphate and energy change in cultured endothelial and $P388D_1$ cells following oxidant injury. J Clin Invest 1985, 76:1471–1476
9. Schraufstatter IU, Hinshaw DB, Hyslop PA, Spragg RG, Cochrane CG: Glutathione cycle activity and pyridine nucleotide levels in oxidant induced injury of cells. J Clin Invest 1985, 76:1131–1139
10. Bellomo G, Jewell SA, Thor H, Orrenius S: Regulation of intracellular calcium compartmentation: Studies with isolated hepatocytes and t-butyl hydroperoxide. Proc Natl Acad Sci USA 1982, 79:6842–6846
11. Trump BF, Mergner WJ: The inflammatory process. 2nd edition. Cell Injury, Vol I. Edited by BW Zweifach, et al. New York, Academic Press, 1974, pp 115–257
12. Jewell SA, Bellomo G, Thor H, Orrenius S, Smith MT: Bleb formation in hepatocytes during drug metabolism is caused by disturbances in thiol and calcium ion homeostasis. Science 1982, 217:1257–1259
13. Scott RE: Plasma membrane vesiculation: A new technique for isolation of plasma membranes. Science 1976, 194:743–745
14. Scott RE, Perkins RG, Axchunke MA, Hoer BJ, Maercklein PB: Plasma membrane vesiculation in 3T3 and SV 3T3 cells: I. Morphological and biochemical characterization. J Cell Sci 1979, 35:229–243
15. Kinn SR, Allen TD: Conversion of blebs to microvilli: Cell surface reorganization after trypsin. Differentiation 1981, 20:168–173
16. Wu E, Tank DW, Webb WW: Unconstrained lateral diffusion of concanavalin A receptors on bulbous lymphocytes. Proc Natl Acad Sci USA 1982, 79:4962–4966
17. Tank DW, Wu E, Webb W: Enhanced molecular diffusibility in muscle membrane blebs: Release of lateral constraints. J Cell Biol 1982, 92:207–212
18. Dang CV, Bell WR, Kaiser D, Wong A: Disorganization of cultured vascular endothelial cell monolayers by fibrinogen fragment D. Science 1985, 227:1487–1490
19. Phillips DR, Jennings LK, Edwards HH: Identification of membrane proteins mediating the interaction of human platelets. J Cell Biol 1980, 86:77–86
20. Howard TH, Meyer WH: Chemotactic peptide modulation of actin assembly and locomotion in neutrophils. J Cell Biol 1984, 98:1265–1271
21. Wallace PJ, Wersto RP, Packman CH, Lichtman MA: Chemotactic peptide-induced changes in neutrophil actin conformation. J Cell Biol 1984, 99:1060–1065

22. Rungger-Brandle E, Gabbiani G: The role of cytoskeletal and cytocontractile elements in pathologic processes. Am J Pathol 1983, 110:361-392
23. Sklar LA, Omann GM, Painter RG: Relationship of actin polymerization and right angle light scattering in human neutrophils: Dependence on receptor occupancy and Ca^{++}. J Cell Biol 1985, 101:1161-1166
24. Hyslop PA, Sklar LA: A quantitative fluorimetric assay for the determination of oxidant production of polymorphonuclear leukocytes: Its use in the simultaneous fluorimetric assay of cellular activation processes. Analytical Biochem 1984, 141:280-286
25. Wulf E, Deboren A, Bantz FA, Faulstich H, Wieland T: Fluorescent phallotoxin, a tool for the visualization of cellular actin. Proc Natl Acad Sci USA 1979, 76:4498-4502
26. Weiland Th, Faulstich H: Amatoxins, phallotoxins, phallolysin, and antamanide: The biologically active components of poisonous Amanita mushrooms. Crit Rev Biochem 1978, 5:185-260
27. Laemmli UK. Cleavage of structural proteins during the assembly of the head of bacteriophage T_4. Nature 1970, 227:680-685
28. Pardee JD, Spudich JA: Purification of muscle actin. Meth Enzymol 1982, 85:164-181
29. Adelstein RS, Eisenberg E: Regulation and kinetics of the actin-myosin-ATP interaction. Ann Rev Biochem 1980, 49:921-956
30. Bershadsky AD, Gelfand VI: Role of ATP in the regulation of stability of cytoskeletal structures. Cell Biol Int Repo 1983, 7:173-187
31. Bershadsky AD, Gelfand VI, Svitkina TM, Tint IS: Destruction of microfilament bundles in mouse embryo fibroblasts treated with inhibitors of energy metabolism. Exp Cell Res 1980, 127:421-429
32. Sanger JW, Sanger JM: Differential response of three types of actin filament bundles to depletion of cellular ATP levels. Eur J Cell Biol 1983, 31:197-204
33. Kirschner MW, Williams RC: The mechanism of microtubule assembly *in vitro*. J Supramol Struct 1974, 2:412-428
34. Kuriyama R, Sakai H: Viscometric demonstration of tubulin polymerization. J Biochem 1974, 75:463-471
35. Shasby DM, Shasby SS: Calcium mediated increases in endothelial permeability: Role of endothelial cell microfilaments (Abstr). Am Rev Respir Dis 1983, 127 (Suppl):306
36. Shasby DM, Shasby SS, Sullivan JM, Peach MJ: Role of endothelial cell cytoskeleton in control of endothelial permeability. Circ Res 1982, 51:657-661
37. Edelhauser HF, Van Horn DL, Miller P, Pederson HJ: Effect of thiol-oxidation of glutathione with diamide on corneal endothelial function, junctional complexes and microfilaments. J Cell Biol 1976, 68:567-578

Acknowledgments

We wish to thank Dr. C.-M. Chang for his expert assistance with the electron microscopy, Donald McQuitty for his assistance with the flow cytometry, and Ms. Dian Caudebec for her excellent secretarial help with the manuscript. Drs. Hinshaw, Schraufstatter, and Hyslop are recipients of fellowships from the American Lung Association, the Puritan-Bennett Foundation, and the American Heart Association, respectively.